

Numerical Optimization on Approach and Landing for Reusable Launch Vehicle

Devanath B.¹, Laila Beebi M.²

¹Department of Electrical and Electronics, TKM College of Engineering, Kollam, India

Abstract: The development of a plane which can fly to space at lower cost, which is reusable and can take more payloads, is very much required for further development of space industries. The Reusable Launch Vehicle, usually called Spaceplane or Hyperplane which can take crew and payload into orbit is being developed by various space agencies and private companies. The Spaceplane would make space travel cheap and will help in increasing space tourism and just like in the aviation industry, within a few decades, the space tourism industries would be worth billions. The objective of this paper is to design a numerically optimized trajectory on approach and landing phase of Reusable Launch Vehicle.

Keywords: Quasi Equilibrium Glide; RLV; Numerical Optimization; Approach and Landing

1. Introduction

Second generation (and future generation) RLVs may eventually take the place of the space shuttles, but not before scientists perfect the technologies that make RLVs safer, more reliable, and less expensive than the shuttle fleet. To achieve this goal, a variety of RLV trajectory design approaches have recently been proposed. Generally, an RLV mission is composed of four major flight phases: ascent, re-entry, terminal area energy management (TAEM), and approach and landing (A&L).

A neural network has been employed for optimal trajectories over the flight conditions in A&L, from which the trajectory to be flown can be reshaped to improve on range flown [1]. Another algorithm was developed for A&L by iteratively seeking to satisfy a final-flare flight-path-angle constraints [3]. An Autoland trajectory design for the X-34 Mach 8 vehicle was presented in Barton and Tragesser (1999). The techniques facilitate rapid design of reference trajectories. The trajectory of the X-34 based on the shuttle approach and landing design was from steep glideslope, circular flare, and exponential flare to shallow glideslope.

The objective of this paper is to develop new approaches that can deliver an RLV to its landing site safely and reliably, recover the vehicle from some failures, and avoid mission abort as much as possible and hence to generate trajectory of an unpowered RLV by implementing numerical optimization during A&L phase of reentry

2. System Model

2.1 Point-mass Equations of Motion

For an unpowered RLV during A&L, the discussion is restricted only to flight in the longitudinal plane. The gliding flight in a vertical plane of symmetry is then defined by the following point mass equations

$$\dot{V} = -\frac{D}{m} - g \sin \gamma \quad (1)$$

$$\dot{\gamma} = \frac{L}{mV} - \frac{g}{V} \cos \gamma \quad (2)$$

$$\dot{h} = V \sin \gamma \quad (3)$$

$$\dot{R} = V \cos \gamma \quad (4)$$

where V is velocity of vehicle, γ is flight-path angle, h is the altitude, R is the down range, L and D are the lift and drag forces, g is the acceleration due to gravity and m is the mass of the vehicle.

Here we select energy height as independent variable for integration instead of time

$$e = \frac{V^2}{2g} + h \quad (5)$$

Energy height is the total mechanical energy of the vehicle divided by its weight.

Hence equations become

$$\frac{dV}{de} = \frac{\dot{V}}{\dot{e}} = \frac{g}{V} + \frac{mg^2}{DV} \sin \gamma \quad (6)$$

$$\frac{d\gamma}{de} = \frac{\dot{\gamma}}{\dot{e}} = -\frac{gL}{DV^2} + \frac{mg^2}{DV^2} \cos \gamma \quad (7)$$

$$\frac{dh}{de} = \frac{\dot{h}}{\dot{e}} = -\frac{mg}{D} \sin \gamma \quad (8)$$

$$\frac{dR}{de} = \frac{\dot{R}}{\dot{e}} = -\frac{mg}{D} \cos \gamma \quad (9)$$

2.2 Aerodynamic Model

The lift and drag forces are,

$$L = \bar{q} S C_L \quad (10)$$

$$D = \bar{q} S C_D \quad (11)$$

Where \bar{q} is dynamic pressure, S is wing surface area, C_L and C_D are lift and drag coefficients. Dynamic pressure is,

$$\bar{q} = \frac{1}{2} \rho V^2 \quad (12)$$

Where ρ is atmospheric density. lift and drag coefficient is defined as

$$C_L = C_{L0} + C_{L\alpha} \alpha \quad (13)$$

$$C_D = C_{D0} + K C_L^2 \quad (14)$$

Where C_{L0} coefficient at zero angle of attack is, C_{D0} is zero-lift drag coefficient, K is induced-drag coefficient, and $C_{L\alpha}$ is "lift slope" coefficient.

$$\frac{L}{D} = \frac{C_L}{C_D} = \frac{C_L}{C_{D0} + K C_L^2} \quad (15)$$

C_L corresponding to maximum L/D is denoted by C_L^* and is

$$C_L^* = \sqrt{\frac{C_{D0}}{K}} \quad (16)$$

Angle of attack for maximum L/D can be now found by substituting C_L^* for C_L

$$\alpha^* = \frac{C_L^* - C_{L0}}{C_{L\alpha}} \quad (17)$$

2.3 Control Model

Given that the purpose of this research is to develop a means of computing a control profile that maximizes the range covered by the vehicle, several possible approaches have been considered for defining the control profile. The only control input considered in this study is angle of attack and, to simplify the model, the dynamics of the control system are neglected—i.e., adjustments in angle of attack are assumed to take place instantaneously. In reality, angle of

Optimal control profiles should closely resemble the maximum- L/D trajectory, which is derived as a simple approximation of the optimal trajectory. In order to highlight the differences between flying at max L/D and flying an optimal trajectory, the original control profile definition was modified so that each control node was defined as a deviation $\delta(\alpha)$ from α^*

$$\alpha(t) = \alpha^*(M) + \delta\alpha(t) \quad (18)$$

It was believed that the optimal angle of attack at a given instant was primarily affected by Mach number, so the control nodes were parameterized in terms of Mach number instead of time

$$\alpha(M) = \alpha^*(M) + \delta\alpha(M) \quad (19)$$

Mach number was not guaranteed to be monotonic, and because the flight dynamics are integrated with respect to energy height, it was finally decided that the control nodes should be parameterized in terms of energy height, which is monotonic:

$$\alpha(e) = \alpha^*(M) + \delta\alpha(e) \quad (20)$$

3. Numerical Optimization

The optimization problem is defined as follows: Find the $\delta\alpha(e)$ profile that minimizes

$$F = -R(e_f) \quad (21)$$

where $R(e_f)$ is the horizontal range flown when the vehicle has reached the final energy height, e_f , and the $\delta\alpha(e)$ profile is defined according to Eq. (20). The value of α at each control node, then, serves as one independent variable in the optimization problem. Equation (21) gives the negative of $R(e_f)$ for use with the MATLAB `fmincon` function because `fmincon` only minimizes objective functions, and the purpose of this optimization is to maximize $R(e_f)$. In order for the terminal states of the trajectory to coincide with the A&L interface, it is possible to set one or more terminal-state equality constraints:

$$C_1(e_f) = V(e_f) - V_f = 0 \quad (22)$$

$$C_2(e_f) = \gamma(e_f) - \gamma_f = 0 \quad (23)$$

$$C_3(e_f) = h(e_f) - h_f = 0 \quad (24)$$

attack cannot be adjusted instantaneously because it is controlled by ailerons that require time to move and because the vehicle requires time to respond to the new control input. The assumption of instantaneous control is adequate, however, for observing basic trends in optimal control profiles, even if those profiles are not continuous or differentiable. A non-differentiable control profile cannot be achieved in reality (where velocity, acceleration, and higher-order rates must all be continuous), but a differentiable curve might be fitted to approximate the non-differentiable profile with little effect on performance of the vehicle. It is assumed that a realistic control system could nearly replicate the control profiles found in this study by use of such an approximation. Hence, the dynamics of the control system are neglected for the purposes of this investigation.

These constraints would increase the computational time to converge on an optimal solution so no terminal states are constrained in this study.

Side constraints are placed on the angle-of-attack deviations $\delta\alpha(e)$ at each control node. The range of acceptable inputs (-6 deg to 21 deg) to the aerodynamic model:

$$-6 - \alpha^*(M) < \delta\alpha(e) < 21 - \alpha^*(M) \quad (25)$$

A. Selection of the Number of Control Nodes

Numerous trials were conducted with different numbers of control nodes to determine the number of nodes that constitutes a good balance between accuracy and computational cost. Each consecutive trial doubled the number of intervals between control nodes from the previous trial, thereby halving the mesh size for the control profile

Hence, if there is only one node in the first trial (i.e., a constant offset from the (α^*) profile), then adding a node to make two nodes in the second trial, then doubling the number of intervals to make three nodes, the following relationship arises:

$$N_i = 1, i = 1 \quad (26)$$

$$N_i = 2, i = 2 \quad (27)$$

$$N_{i+1} = N_i + (N_i - 1) = 2N_i - 1, i > 2 \quad (28)$$

Where N_i is the number of control nodes in the i th trial. This relationship produces the following sequence of numbers of control nodes: 1, 2, 3, 5, 9, 17, 33, 65, 129, etc.

4. Results

Simulation is carried out using MATLAB. Taking 17 nodes for numerical optimization and initial velocity is chosen as $V_0 = 439$ ft/s and a deviation of +60 ft/s (case2) and -60 ft/s (case3) is taken

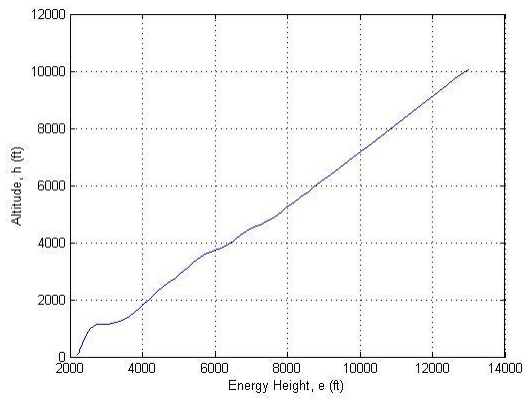


Figure 1: Altitude Vs. energy height for case1

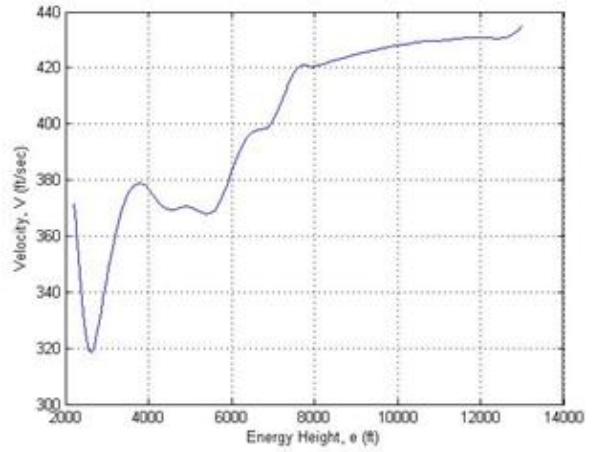


Figure 4: Velocity Vs. energy height for case1

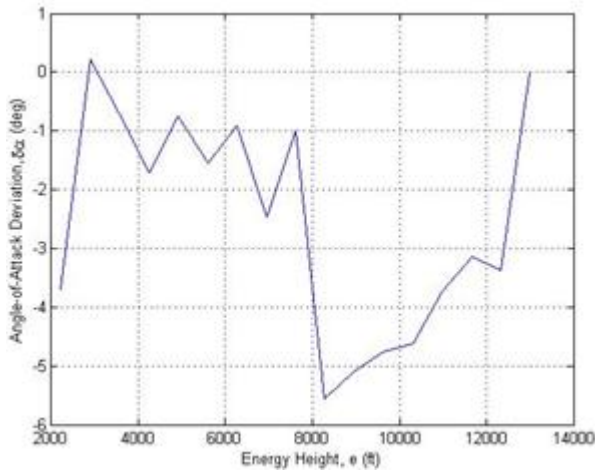


Figure 2: Angle-of-attack Deviation Vs. energy height for case1

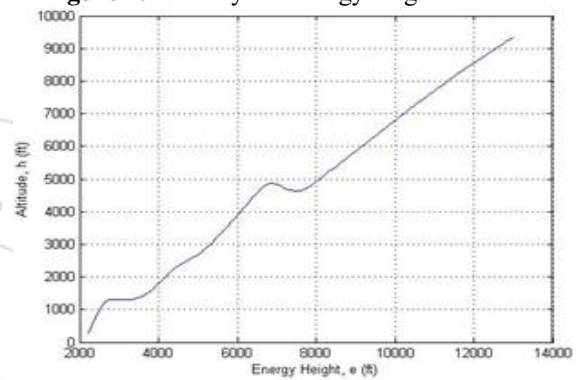


Figure 5: Altitude Vs. energy height for case2

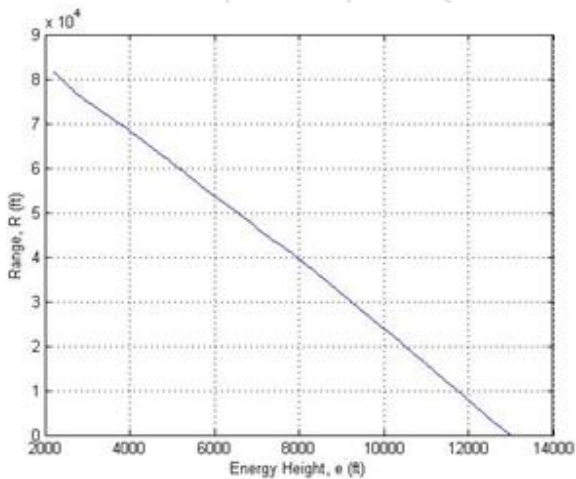


Figure 3: Range Vs. energy height for case1

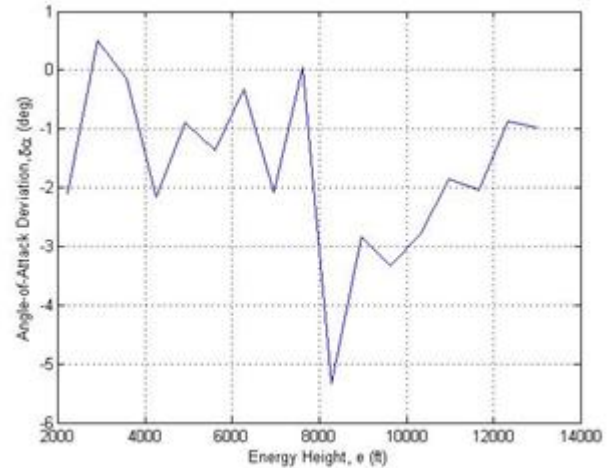


Figure 6: Angle-of-attack Deviation Vs. energy height for case2

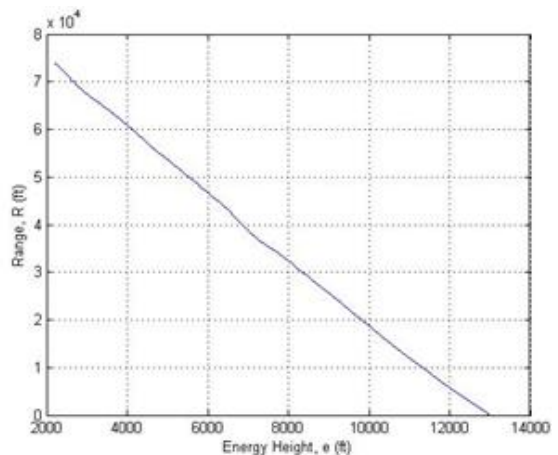


Figure 7: Range Vs. energy height for case2

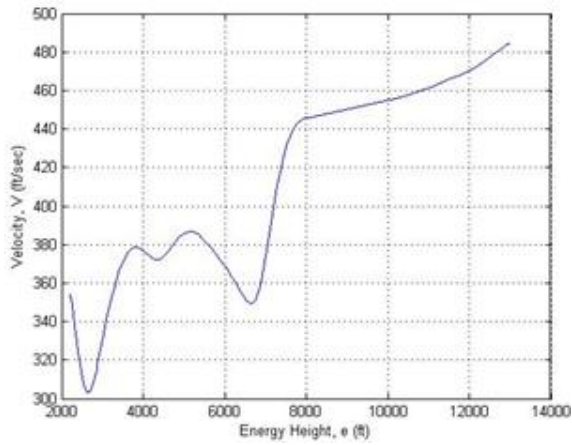


Figure 8: Velocity Vs. energy height for case2

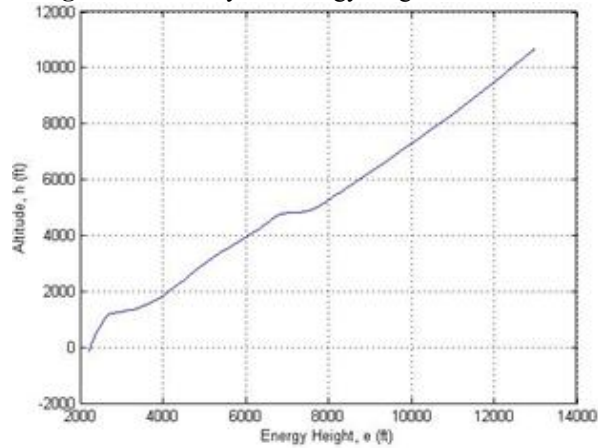


Figure 9: Altitude Vs. energy height for case3

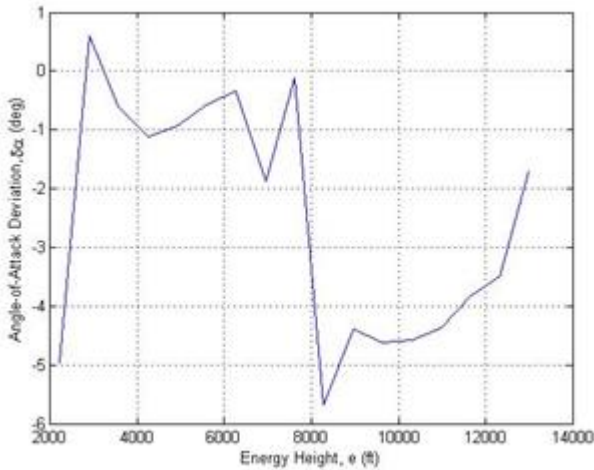


Figure 10: Angle-of-attack Deviation Vs. energy height for case3

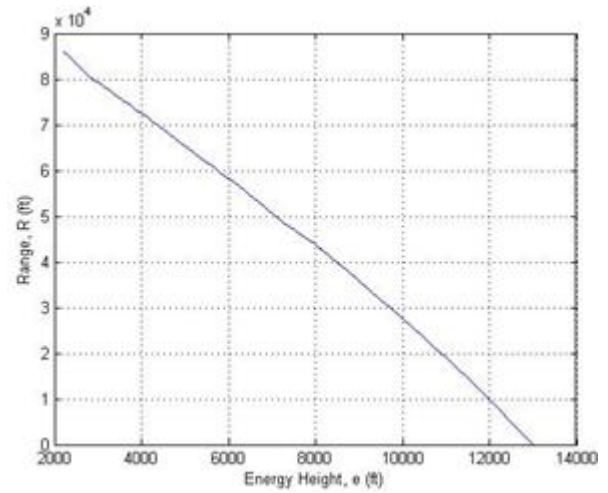


Figure 11: Range Vs. energy height for case3

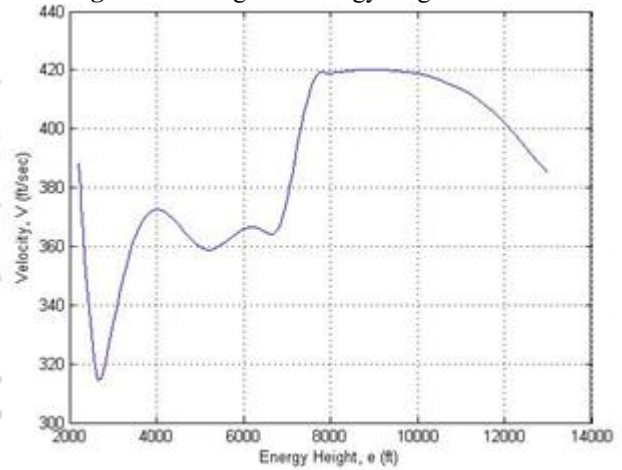


Figure 12: Velocity Vs. energy height for case3

Table 1: Nominal parameters for constant drag polar aerodynamic model

Parameter	Value
Zero-Angle Lift Coefficient, C_{L0}	0.11502
Lift-Slope Coefficient, $C_{L\alpha}$	0.051718
Zero-Lift Drag Coefficient, C_{D0}	0.021348
Induced Drag Coefficient, K	0.26647

5. Conclusion

A higher-order interpolation method might also improve the realism of the control profile by making it more feasible to employ with real control surfaces, given that real control surfaces cannot respond instantly to control commands. For that matter, it might be helpful to include the pitch control dynamics of the vehicle in the simulation model, rather than assuming the vehicle can adjust its angle of attack instantaneously. These unmodeled details could affect the optimization of the control profile. Along with other methods of interpolating between control nodes, it may be desirable to consider non uniform distributions of nodes along the trajectory, placing more nodes in areas needing higher resolution (e.g., at energy heights for which velocity is transonic), improving the range of the vehicle without the computational expense of increasing the number of control nodes.

6. Acknowledgment

The authors wish to acknowledge Dr. Josiah Bryan in the Mechanical and Aerospace Engineering Department at the University of Missouri for providing helpful suggestions and his comments on this paper.

References

- [1] Schierman, J. D., Hull, J. R., and Ward, D. G., —“Adaptive Guidance with Trajectory Reshaping for Reusable Launch Vehicles,” AIAA, August 2002, paper 02-4458.
- [2] Barton, G. H., and Tragesser, S. G., —“Attolanding Trajectory Design for the X-34,” AIAA, August 1999, paper 99-4161.
- [3] Kluever, C. A., —“Unpowered Approach and Landing Guidance Using Trajectory Planning,” *Journal of Guidance, Control, and Dynamics*, 2004, 967-974.
- [4] De Ridder, S., —“Optimal Longitudinal Trajectories for Reusable Space Vehicles in the Terminal Area,” *Journal of Spacecrafts and Rockets*, 2011, 642-653
- [5] Josiah Bryan., —“Maximum-range Trajectories for an Unpowered Reusable Launch Vehicle,” *mospace*, 2011
- [6] De Ridder, S., —“Optimal Longitudinal Trajectories for Reusable Space Vehicles in the Terminal Area,” *Journal of Spacecrafts and Rockets*, 2011, 642-653
- [7] Hull, J. R., Gandhi, N., and Schierman, J. D., —“In-Flight TEAM/Final Approach Trajectory Generation for Reusable Launch Vehicles,” AIAA, September 2005, paper 2005-7114.
- [8] M. L. Xu, K. J. Chen, L. H. Liu, and G. J. Tang, —“Quasiequilibrium glide adaptive guidance for hypersonic vehicles,” *Science China Technological Sciences*, vol. 55, pp. 856–866, 2012.
- [9] Kluever, C. A., and Horneman, K. R., August 2005, —“Terminal Trajectory Planning and Optimization for an Unpowered Reusable Launch Vehicle,” AIAA Paper 2005-6058.
- [10] Burchett, B. T., —“Fuzzy Logic Trajectory Design and Guidance for Terminal Area Energy Management,” *Journal of Spacecraft and Rockets*, 2004, pp. 444-450.
- [11] Kluever, C. A., —“Terminal Guidance for an Unpowered Reusable Launch Vehicle with Bank Constraints,” *Journal of Guidance, Control, and Dynamics*, 2007, pp. 162-168.
- [12] Baek, J., Lee, D., Kim, J., Cho, K., and Yang, J., —“Trajectory optimization and the control of a re-entry vehicle in TAEM phase,” *Journal of Mechanical Science and Technology*, 2008, pp. 1099-1110.
- [13] C. Weiland, *Computational Space Flight Mechanics*, Springer, 2010.

Author Profile



Devanath B. received the B.tech. in Electrical Engineering from College of Engineering and Management, Punnapra in 2013 (under University of Kerala) and now pursuing M.Tech degree from TKM College of Engineering, kollam.



Laila Beebi M. obtained her M.Tech in Guidance and Navigation from College of Engineering, Trivandrum and B.E. degrees from T K M College of engineering, Kollam, Kerala, in 1982 and 1998 respectively. She's got 25 years of teaching experience and is currently working as the Head of the Department of Industrial Instrumentation and Control (M Tech) of the Electrical and Electronics Department of T K M College of engineering, Kollam, Kerala, India